coatings

MDPI

Article

A Study on the Improvement of the Photothermal Characteristics of the Adsorbent for Sorption-Based Atmospheric Water Harvesting Driven by Solar

Jiangbo Wu, Ziyi Sui, Xiaoze Du *, Yaocong Zhang and Tao Ma

School of Energy and Power Engineering, Lanzhou University of Technology, Lanzhou 730050, China
* Correspondence: duxz@ncepu.edu.cn; Tel.: +86-(10)-61773923

Abstract: Facing the global freshwater resource crisis, using solar energy to produce fresh water resources in an environmentally friendly way, sorption-based atmospheric water harvesting driven by solar technology has attracted increasingly more attention. In the current research, the adsorbent MOF-801 has the advantages of a high adsorption capacity and is suitable for fields with a wide range of humidity. However, the strong interaction between the adsorbent and water molecules is conducive to rapid moisture absorption, but at the same time, the adsorbent needs higher heat to achieve regeneration, which restricts the practical application of the adsorbent. Based on the principle that carbon materials can improve the photothermal conversion performance of adsorbent, this paper prepared three composite adsorbents with MOF-801 and three different carbon materials, characterized the structure and morphology of each adsorbent, and compared the effects of different carbon materials on the performance of MOF-801 adsorbent. Among them, the photothermal characteristics of MOF-801/CNT adsorbent proposed in this paper are most significantly improved. The experiment shows that compared with MOF-801/G, the adsorption capacity is increased by 30%, and the desorption speed is increased by 50%. It maximizes water withdrawals over a period of time in arid environments.

Keywords: atmospheric water harvesting; carbon nanotubes; MOF-801 adsorbent; photothermal characteristic

Citation: Wu, J.; Sui, Z.; Du, X.; Zhang, Y.; Ma, T. A Study on the Improvement of the Photothermal Characteristics of the Adsorbent for Sorption-Based Atmospheric Water Harvesting Driven by Solar. *Coatings* **2023**, *13*, 154. https://doi.org/10.3390/coatings13010154

Academic Editor: Maciej Fronczak

Received: 15 December 2022
Revised: 8 January 2023
Accepted: 9 January 2023
Published: 11 January 2023

1. Introduction

According to a study, about 2.3 billion people in the world live in countries where water resources are scarce, and 785 million people cannot even be guaranteed the most basic drinking water [1]. With the development of human economy and society, industrial pollution [2] and agricultural production [3] will also lead to the shortage of freshwater resources becoming more acute. The regions facing the shortage of water resources in the world generally have very rich solar energy resources [4]. Solar energy resources are renewable, clean, and pollution-free, and are not subject to geographical restrictions. Therefore, more and more scholars are exploring the use of local abundant solar energy resources in water shortage areas to produce renewable fresh water resources. Nature has predicted that the solar-driven, sorption-based atmospheric water harvesting technology is expected to solve the water shortage problem of 1 billion people in arid regions of the world in the future [5]. The sorption-based atmospheric water harvesting method breaks away from the restriction of electric power, and is suitable for various extreme climates. It has the characteristics of the widest application scenarios and the greatest potential. Therefore, increasingly more scholars are paying attention to and studying the sorption-based atmospheric water harvesting technology.

The performance of the adsorbent fundamentally determines and limits the water abstraction efficiency of an atmospheric water harvesting system. The ideal adsorbent should have the characteristics of high moisture absorption, fast moisture absorption speed,

wide working field (moisture absorption can increase with the increase in humidity in a wide humidity range), efficient and fast desorption driven by relatively low-temperature heat sources such as solar energy, and high cycle life [6]. Based on the research status of various adsorbents in recent years, it can be found that although the water yield of zeolite [7,8] and silica gel [9,10] is moderate among solid adsorbents, it is not suitable for the atmospheric water harvesting system, because zeolites have high desorption temperatures, high energy consumption for regeneration, and long working cycles. Meanwhile, silica gel has a low total pore space volume and limited adsorption force, resulting in a generally larger system volume. For hygroscopic salts [11,12], the performance is difficult to regulate, and is prone to cause system corrosion and other problems, because it will dissolve in the prepared water. Usually, the solution to this problem is to encapsulate the hygroscopic salt into other matrices, but which leads to reduced absorption kinetics and poor stability.

MOFs [13,14] (Metal Organic Frameworks) are more suitable for application in an atmospheric water harvesting system and are expected to overcome the shortcomings of the above adsorbents. Its pore structure and chemical properties can be regulated at the molecular level by different ligands allowing it to maintain a high humidity absorption speed and high humidity absorption amount in low temperature and drought environments, but the desorption temperature is still high and the solar energy utilization efficiency is low. Yaghi's team [14,15] reported MOF-801 adsorbent with excellent adsorption properties in *Science*. The MOF-801 is composed of 12 connected Zr-based clusters $Zr_6O_4(OH)_4(\text{-}COO)_{12}$ joined by fumarate linkers into a three-dimensional, extended porous framework of fcu topology. The structure of MOF-801 contains three symmetrically independent cavities into which water molecules can be captured and concentrated. However, the desorption temperature of pure MOF-801 is extremely high. In order to achieve atmospheric water harvesting driven by low-temperature heat sources such as solar energy, MOF-801 and graphite (G) were mechanically stirred and mixed in a wide-mouth bottle to prepare MOF-801/G, which reduced the desorption temperature and achieved multiple adsorption and desorption cycles within one day, successfully increasing water production. Although their work on MOF-801 is comprehensive, the research on adding carbon materials to improve the photothermal properties of adsorbents is not in-depth. As each carbon material has different light absorption and thermal conductivity, there will be a big gap in improving the photothermal performance of the adsorbent. On this basis, if a carbon material with better photothermal properties than graphite is added, it is expected to develop a new composite adsorbent with higher light absorption degree and photothermal conversion rate. In this work, we synthesized high water-adsorbed photothermal composite consisting of MOF-801 and carbon nanotubes (CNT). This composite adsorbent demonstrates nice water adsorption capacity and fast adsorption and desorption. This strategy sheds light on the development of photothermal adsorbents for water capture with easy regeneration.

2. Experimental Section

2.1. Selection of Composite Adsorbent Materials and Mixing Ratio

In terms of material selection, the addition of different carbon materials has different effects on the adsorption and photothermal properties of the adsorbent. It is hoped that the carbon material with the best coordination effect with MOF-801 adsorbent can be found among common carbon materials to prepare a new composite adsorbent.

MOF-801 with high adsorption capacity and a wide humidity adsorption field, but poor photothermal conversion, long desorption time and high energy consumption was selected as the adsorption substrate. The common carbon-based materials graphite (G), carbon black powder (CB), and carbon nanotubes (CNT) were selected as additives to improve the photothermal properties. MOF-801/G prepared using G was the control group for composites. The purpose is to compare the adsorption and desorption properties of three composite adsorbents MOF-801/CNT, MOF-801/G and MOF-801/CB, and to select an efficient adsorbent with excellent humidity absorption and desorption properties.

It can also be compared with the existing studies by Yaghi's team [14,15] to verify the experimental accuracy.

In the selection of the mixing ratio, the 67:33 wt% mixing ratio proved to be feasible in the Yaghi team [14,15] study and was used as the proportion of MOF-801 and carbon material components in the composite adsorbent.

2.2. Composite Adsorbent Preparation Method

In order to make the MOF-801 adsorbent and carbon material mix more evenly, the ball mill instrument (QM-3SP04, nju-instrument, Nanjing, China) was used for wet ball milling to compound, compared with the method of Yaghi's team [14,15] using a wide-mouth bottle shake. CNT, G, CB, and MOF-801 were added to the agate ball mill tank according to the ratio of 67:33 wt%, respectively. Zirconia beads were used as grinding beads and methanol was used as dispersion to grind and mix. The mixed suspension was frozen at −40 °C and then vacuum freeze-dried for 3 days at a pressure of <10 Pa in a vacuum freeze dryer. Three composite desiccants, namely MOF-801/CNT, MOF-801/G, and MOF-801/CB, were prepared after freeze-drying.

In order to empty the methanol molecules remaining in pore canal and other impurity molecules from the atmosphere, MOF-801 and three composite adsorbents need to be activated before use, and activated for 12 h at 120 °C using a vacuum drying closet.

2.3. Characterization

Scanning electron microscopy (SEM) images were recorded on a Tescan MIRA LMS (Kohoutovice, Czech Republic). The powder X-ray diffraction data (XRD) were collected on X-ray powder diffractometers (Rigaku D MAX-2600, Tokyo, Japan) using Cu Kα radiation sources. The Fourier transform infrared (FTIR) spectra were carried out on a Thermo Scientific Nicolet iS20 device (Waltham, MA, USA) using KBr pellets in the wavenumber range of 400–4000 cm^{-1}. N_2 sorption isotherms were measured by a Micromeritics ASAP 2460 (Micromeritics Instrument, Norcross, GA, USA). UV–vis-NIR spectra were recorded on a PerkinElmer Lambda1050 (Waltham, MA, USA). The chambers for experiments with constant temperature and humidistat (Aikosp, Nanjing, China) was used to control temperature humidity. A xenon lamp light source (PLS-SXE300D/UV, PerfectLight, Beijing, China) was used to generate the simulated sunlight.

2.4. Water Sorption

In order to explore the influence of different carbon materials, temperature, and humidity on the adsorption performance of composite adsorbent, the control variable method was used to carry out adsorption experiments on each adsorbent in different environments. Before water sorption assessment, the four adsorbents were weighed at 200 mg and placed in a 35 mm diameter petri dish, the petri dish was placed in a vacuum drying oven at 120 °C and activated for 12 h, and vacuum degree was set to 133 Pa. The analytical balance was placed in the chambers for experiments with constant temperature (T = 5 °C, 15 °C, 25 °C, and 35 °C) and humidistat (RH = 20%, 40%, 60%, and 80%). After activation, the petri dish was removed and placed on the tray of the analytical balance to record the quality change of the adsorbent. The change in reading of the analytical balance is the quality change of the adsorbent during the adsorption process under the temperature and humidity conditions. When the quality of the analytical balance does not change, the adsorbent is adsorbed to saturation.

2.5. Water Release

In order to explore the desorption rate and photothermal conversion temperature of the composite adsorbent after adding different kinds of carbon materials, under the same irradiation intensity, desorption experiments were carried out on the four adsorbents until complete desorption. The four adsorbents were activated in a vacuum drying closet for 12 h, and then placed in a chamber with constant temperature and humidity (T = 25 °C,

RH = 60%) to be saturated. Real sunlight was simulated by a xenon lamp with a 1.5AM filter, and the adsorbent was tested in an environment with a radiation intensity of E = 1 kW/m^2 until it is completely desorbed. The changes in temperature and mass were recorded using a balance and thermocouple.

3. Results and Discussion

3.1. Structure and Morphology Characterization

The SEM images provide the most intuitive display of the structure of the mixed material, as shown in Figure 1. The SEM images of the three composite adsorbents are shown in Figure 1. It can be proved that MOF-801 and the three carbon materials are uniformly mixed.

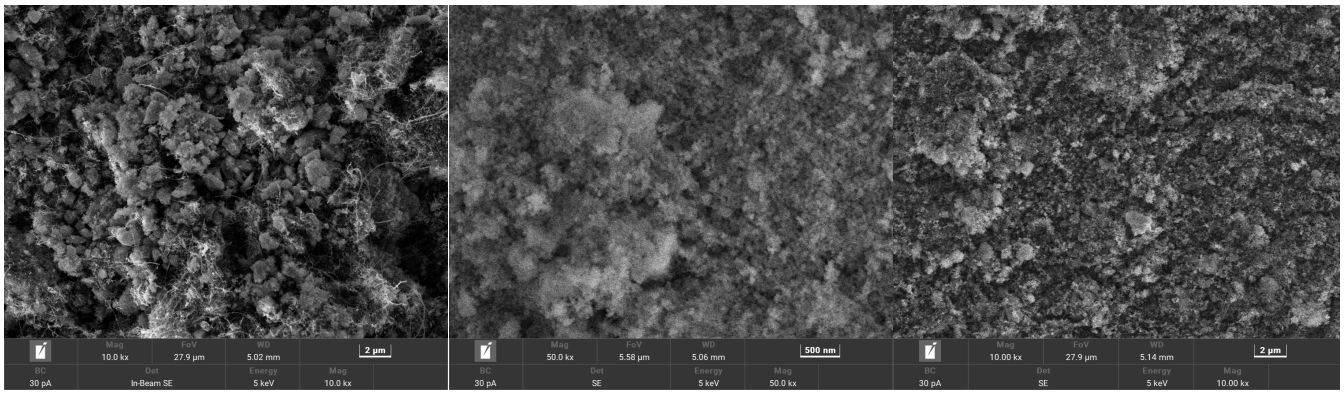

(**a**) (**b**) (**c**)

Figure 1. SEM images of composite adsorbent. (**a**) SEM images of MOF-801/CNT. (**b**) SEM images of MOF-801/G. (**c**) SEM images of MOF-801/CB.

The activated MOF-801/G, MOF-801/CB, and MOF-801/CNT were characterized by X-ray powder diffractometers. The XRD pattern is shown in Figure 2. The peaks at 26.5° correspond to the reflections of CNT, CB, and G, respectively, which are basically consistent with the diffraction peaks of MOF-801. That is, the XRD pattern confirms that the addition of the three carbon materials does not interfere with the crystal structure, but affects the diffraction intensities.

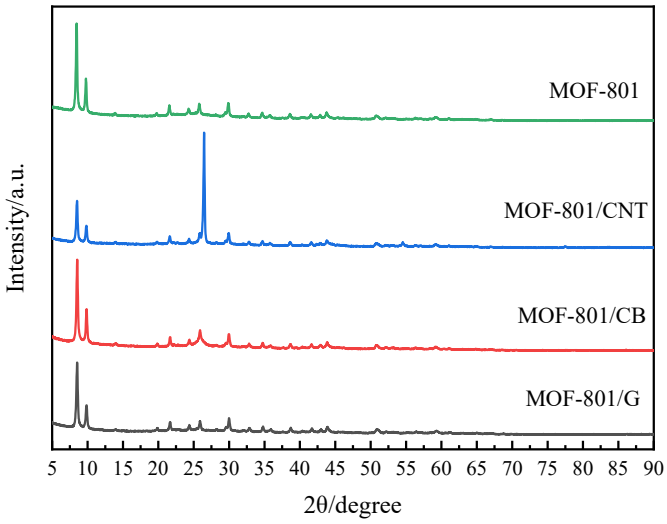

Figure 2. XRD Image of MOF-801, MOF-801/CNT, MOF-801/G, and MOF-801/CB.

The FTIR spectra are shown in Figure 3. After adding carbon materials, there is no significant difference between the FTIR spectra of composites and the peak of MOF-801,

indicating that there is no chemical interaction between MOF-801 and the three carbon materials, only physical mixing. These results indicate that MOF-801 in the composite adsorbent has an adsorption effect, and carbon materials only act as photothermal agents.

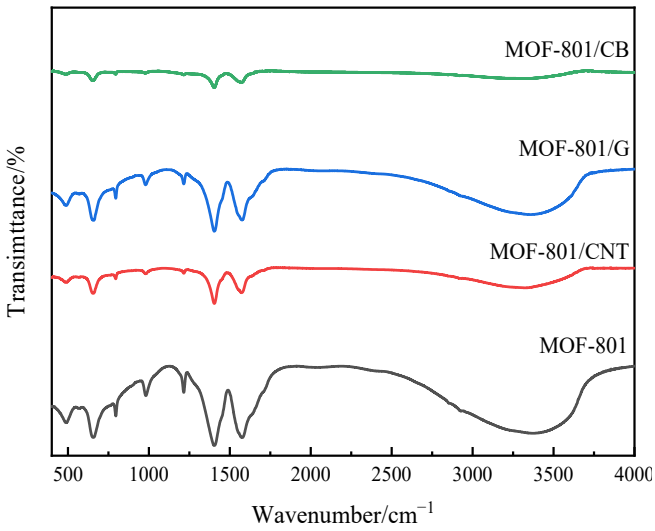

Figure 3. FTIR Image of MOF-801, MOF-801/CNT, MOF-801/G, and MOF-801/CB.

The BET specific surface area, pore volume, average pore size, and other adsorption performance parameters of the four adsorbents can be measured by specific surface and porosity analyzer (BET), as shown in Table 1. At the same time, the adsorption isotherms of four adsorbents under the 77K N_2 atmosphere can also be measured, as shown in Figure 4. For an adsorbent, a good adsorption isotherm type is the basis for an excellent adsorbent, and its equilibrium adsorption capacity can also be uniquely determined by the adsorption curve. The results show that three kinds of composite adsorbents have good potential as adsorbents for an atmospheric water harvesting system.

Table 1. Comparison of adsorbent microstructure size.

Adsorbent	BET Surface Area/m^2/g	t-Plot Micropore Volume/cm^3/g	Average Adsorption Pore Size/nm
MOF-801	511.49	0.136	3.38
MOF-801/CNT	354.77	0.0842	4.26
MOF-801/G	270.68	0.0698	3.92
MOF-801/CB	486.45	0.0896	4.26

It can be seen from Table 1 that compared with MOF-801, the specific surface area and micropores' pore volume of the three composite adsorbents decreased, and the average pore size of the adsorption increased. The reason is that carbon particles with smaller particle size are adsorbed into the pore canal during ball milling mixing, resulting in a decrease in porosity, especially the volume of micropores.

In the adsorption isotherms of the four adsorbents under 77K N_2 atmosphere, as shown in Figure 4, all isotherms showed type I adsorption when P/P_0 was less than 0.1 low-pressure section, and the N_2 adsorption capacity increased sharply with the increase in relative pressure P/P_0, indicating that there were a large number of micropores in the four adsorbents. In the medium pressure range of $0.3 \leq P/P_0 \leq 0.8$, the N_2 adsorption capacity continued to increase with the increase in relative pressure P/P_0, but the increasing tendency slowed down. MOF-801/CB first appeared as a hysteresis loop parallel to the x-axis at $P/P_0 = 0.4$, and the other three materials appeared hysteresis loop at $P/P_0 = 0.8$. It shows that the pore size distribution range of the four adsorbents is wide, and they also have a narrow mesoporous pore. In addition, the particle size of CB in MOF-801/CB is

the largest, the blockage of pore canal is the lightest, the porosity is higher, and the N_2 adsorption capacity is the highest.

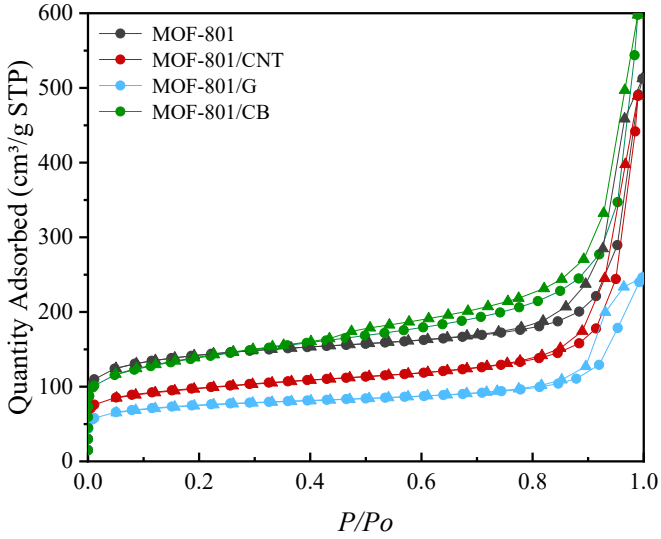

Figure 4. The N_2 sorption isotherms at 77 K of MOF-801, MOF-801/CNT, MOF-801/G, and MOF-801/CB.

3.2. Effects of Different Carbon Materials on the Adsorption Properties of Composite Adsorbents

The adsorption properties of adsorbent mainly include adsorption rate and saturated adsorption capacity. The four adsorbents were adsorbed to saturation at temperature T = 25 °C and relative humidity RH = 20%. The experimental results are shown in Figure 5. It can be seen that MOF-801 reached saturation at 9500 s, the quality change was 21.9%, and the adsorption capacity was 0.219 kg water per kilogram of MOF, recorded as 0.219 kg/kg. MOF-801/CNT reached saturation at 7500 s, the quality change was 16.1%, and the adsorption capacity was 0.161 kg/kg. MOF-801/CB also reached saturation at 7500 s, with a quality change of 14.6% and an adsorption capacity of 0.146 kg/kg. MOF-801/G reached saturation at 7000 s, the quality change was 12.3%, and the adsorption capacity was 0.123 kg/kg. The adsorption capacity of MOF-801 and MOF-801/G is consistent with the research of the Yaghi team [14,15].

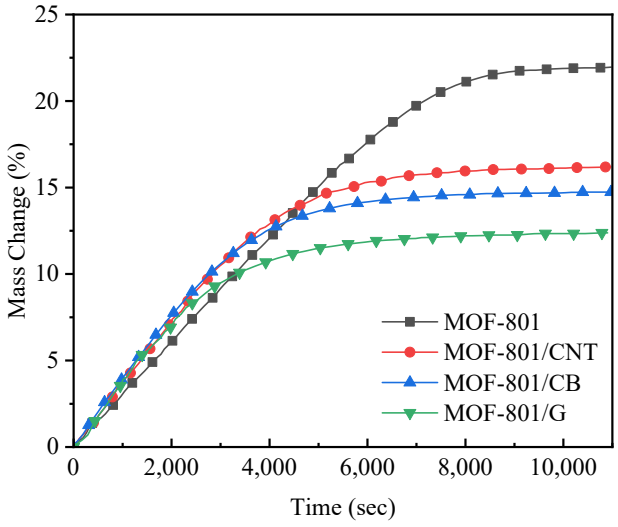

Figure 5. Adsorption curve of MOF-801, MOF-801/CNT, MOF-801/G, and MOF-801/CB at T = 25 °C and RH = 20%.

In summary, in terms of the saturated adsorption capacity of the adsorbent, the ad-sorption capacity of MOF-801/CNT decreased the least among the three composite adsor-bents added with carbon materials for improving photothermal properties. Its adsorption capacity decreased by 25% compared with MOF-801 as the adsorption substrate. The ad-sorption capacity of MOF-801/CB and MOF-801/G decreased by 33% and 44%, respective-ly. In terms of adsorption rate of the adsorbents, MOF-801/CNT adsorption rate was the fastest among the three composite adsorbents, followed by MOF-801/CB and MOF-801/G being the slowest. However, the adsorption rates of all three composites were higher than that of MOF-801 before 3000 s. This indicates that the addition of carbon materials decreased the saturation adsorption capacity but increased the adsorption rate at the initial stage, and MOF-801/CNT had the highest saturated adsorption capacity and adsorption rate, i.e., the best adsorption performance, among the three composites.

3.3. Effects of Humidity on the Adsorption Properties of Composite Adsorbents

The four adsorbents were adsorbed to saturation at different humidity levels (*RH* = 20%, 40%, 60%, and 80%). The experimental results are shown in Figure 6a. When the temperature was 25 °C, with the increase in humidity, the saturated adsorption capacity of MOF-801 gradually increased, the adsorption rate increased, and the time required to reach saturation decreased. The best adsorption characteristics appeared in the working conditions of *T* = 25 °C and *RH* = 80%. After 6000 s, the material adsorbed water to saturation, and the saturated water absorption was 0.272 kg/kg. In sum, for the same kind of adsorbent, the adsorption characteristics of the adsorbent are better in the environment of high humidity.

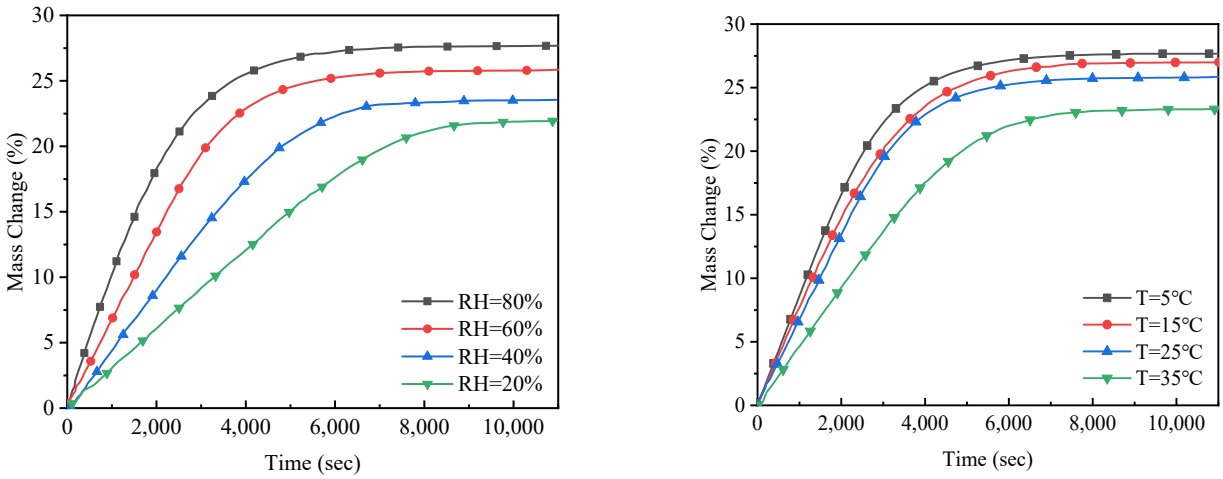

Figure 6. Adsorption curve of MOF-801 at different humidity and temperature. (**a**) Adsorption curve of MOF-801 at *T* = 25 °C and different humidity. (**b**) Adsorption curve of MOF-801 at *RH* = 60% and different temperatures.

In order to further verify this conclusion, and characterize in detail the adsorption performance of MOF-801/CNT, which has the best adsorption performance among the three composite materials, under different temperature and humidity, theMOF-801/CNT was similarly subjected to adsorption experiments under the conditions of *RH* = 60%, *T* = 5 °C, 15 °C, 25 °C, and 35 °C. The experimental results are shown in Figure 7a. It can be seen that the adsorption properties of MOF-801/CNT are better under high humidity, which is consistent with the above conclusion. The best adsorption characteristics appeared in the working condition of *T* = 25 °C and *RH* = 80%. After 5500 s, the material adsorbed water to saturation, and the saturated water absorption was 0.181 kg/kg.

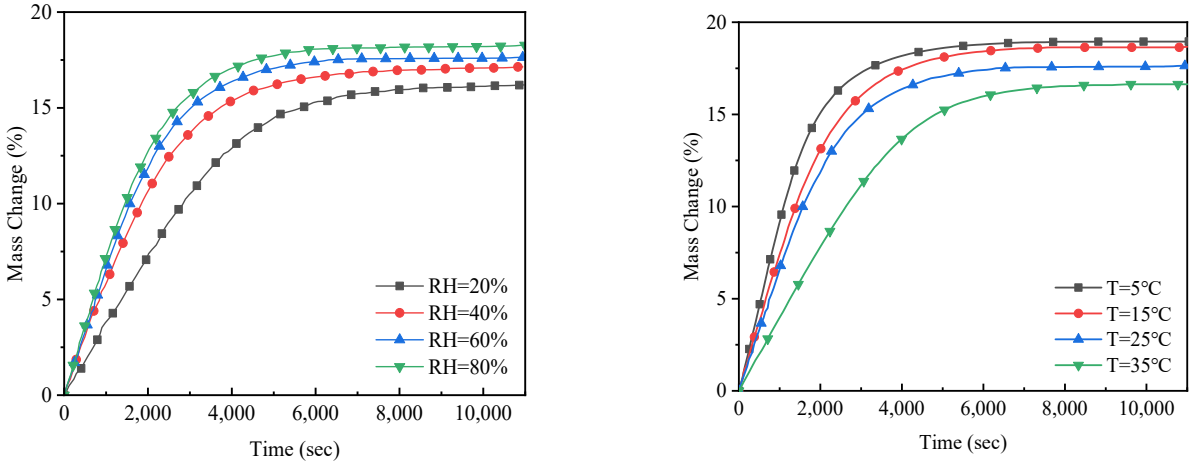

Figure 7. Adsorption curve of MOF-801/CNT at different humidity and temperature. (**a**) Adsorption curve of MOF-801/CNT at T = 25 °C and different humidity. (**b**) Adsorption curve of MOF-801/CNT at RH = 60% and different temperatures.

3.4. Effects of Temperature on the Adsorption Properties of Composite Adsorbents

The four adsorbents were adsorbed to saturation at different temperatures (T = 5 °C, 15 °C, 25 °C, and 35 °C). The experimental results are shown in Figure 6b. When the relative humidity was constant, as the temperature increased, the saturated adsorption capacity of MOF-801 gradually decreased, and the adsorption rate slowed down and the time required to reach saturation increased. This result is also consistent with the research of Yaghi team [14,15]. The best adsorption characteristics appeared in the working condition of T = 5 °C and RH = 60%. After 6500 s, the material adsorbed water to saturation, and the saturated water absorption was 0.276 kg/kg. In summary, for the same adsorbent, the adsorption properties of the adsorbent are better at low temperature.

In order to further verify this conclusion, the adsorption properties of MOF-801/CNT with the best adsorption properties in three composites under different temperature and humidity environments were characterized in detail. The experimental results are shown in Figure 7b. It can be seen that the adsorption properties of MOF-801/CNT are better under lowering the temperature, which is consistent with the above conclusions. The best adsorption characteristics appeared in the working condition of T = 5 °C and RH = 60%. After 5000 s, the material adsorbed water to saturation, and the saturated water absorption was 0.188 kg/kg.

3.5. Light Absorption Properties of Composite Adsorbent Desorption

The photothermal properties of the composite adsorbent include two aspects: optical absorption and photothermal conversion. The optical absorption represents the solar energy absorption and utilization of the adsorbent, and the photothermal conversion performance represents the ability of the adsorbent to convert the absorbed solar energy into the heat energy required for water desorption.

In order to test the light absorption performance of the composite material, the absorption spectra of four kinds of adsorbents were measured. UV–vis-NIR spectra of MOF-801, MOF-801/CNT, MOF-801/G, and MOF-801/CB are shown in Figure 8. The absorption of pure MOF-801 in the 0–2500 nm range fluctuates greatly, and the optical absorption is less than 20% in the 500–2000 nm range. The light absorption fluctuation of the three composite adsorbents is small in the 0–2500 nm range, and the light absorption of MOF-801/G, MOF-801/CB, and MOF-801/CNT are 35%, 50%, and 65%, respectively. These results indicated that the light absorption capacity of the three composite adsorbents was stronger than that of MOF-801 in most spectral ranges. The unique tubular hollow structure of CNT could extend the light path through multiple reflections and confine the light to a small

volume, thus enhances the interaction of light with the materials significantly [16]. Therefore, the light absorption capacity of MOF-801/CNT is the strongest among the composite adsorbents.

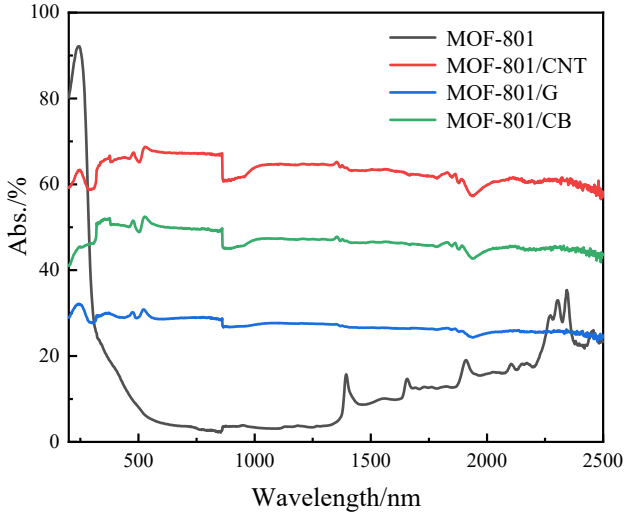

Figure 8. The light absorption curves of MOF-801, MOF-801/CNT, MOF-801/G, and MOF-801/CB.

3.6. Photothermal Conversion Properties of Composite Adsorbent Desorption

The desorption experiment of four kinds of adsorbents was carried out. The experimental results are shown in Figure 9. After adding carbon materials, the water desorption rates of the three composite adsorbents were significantly increased. Among the three composite adsorbents, MOF/CNT has the fastest desorption speed, releasing more than 90% of the water content in 10 min, and releasing the most water content when the desorption is completed in 15 min. It is because of CNT shows the best photothermal conversion ability and thermal conductivity under the same light intensity, which makes the internal temperature of adsorbent rise fastest, reaching 96 °C. Therefore, the higher desorption temperature shortens the desorption time of the adsorbent and improves the known absorption. In sum, among the three composite adsorbents, MOF-801/CNT has the best desorption characteristics.

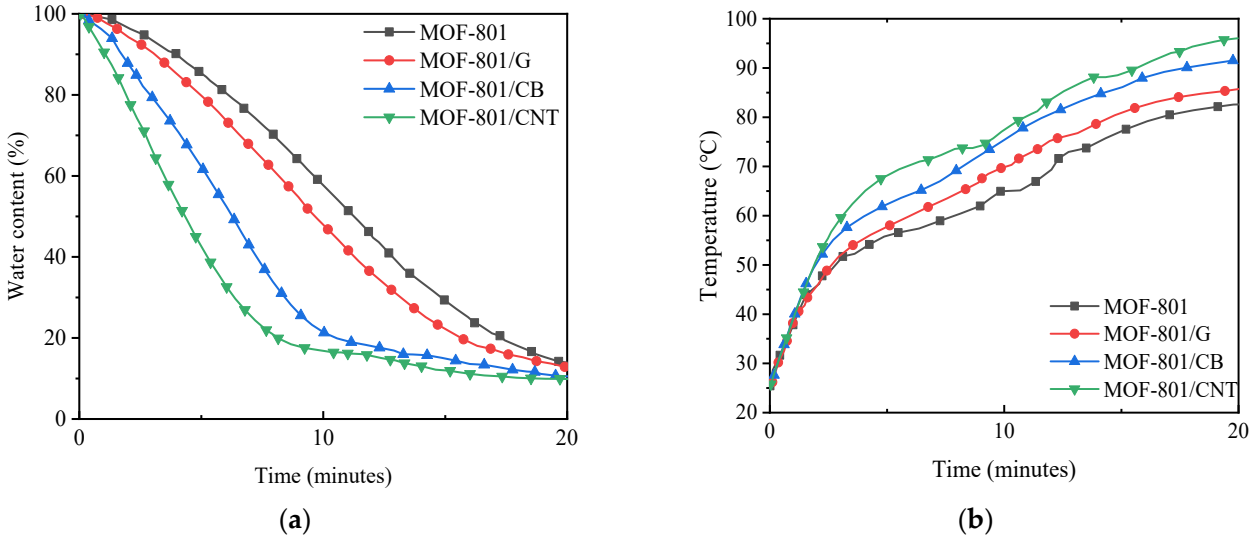

Figure 9. Water content and temperature change profiles of four adsorbents irradiated under 1 kW/m^2 simulated sunlight. (**a**) Desorption curves of four adsorbents under one sun illumination. (**b**) Internal temperature of four adsorbents during desorption.

4. Conclusions

Based on the principle that carbon materials can improve the photothermal conversion performance of adsorbents, the structure and properties of composite adsorbents with different carbon materials were analyzed and characterized. A new composite adsorbent, MOF-801/CNT, was proposed and prepared, which had better adsorption and desorption characteristics than the existing MOF-801/G adsorbent, and the following conclusions have been drawn:

(1) The new composite adsorbent MOF-801/CNT prepared in this paper has better adsorption and desorption properties than the existing MOF-801/G adsorbent. In terms of adsorption properties, the saturated adsorption capacity of MOF-801/CNT was 30% higher than that of MOF-801/G at the same temperature and humidity, and the humidity absorption rate was increased. In terms of desorption characteristics, under the same light intensity, MOF-801/CNT has the best light absorption performance and photothermal conversion performance, the desorption speed is 50% higher than MOF-801/G, and the water release is improved.

(2) The structure and morphology of MOF-801/CNT adsorbent were clarified. The BET specific surface area was 354.77 m^2/g, and the average pore size of the adsorption was up to 4.26 nm, which has excellent qualities as an adsorbent.

(3) The effects of temperature and relative humidity on the adsorption properties of MOF-801/CNT were clarified, that is, the low temperature and high humidity environment are beneficial to improve the adsorption properties of the adsorbent.

Author Contributions: Investigation, Z.S. and J.W.; data curation, Z.S. and J.W.; visualization, Z.S. and Y.Z.; Writing-original draft preparation, Z.S. and Y.Z.; project administration, X.D.; funding acquisition, J.W. and X.D.; resources, X.D.; supervision, T.M. All authors have read and agreed to the published version of the manuscript.

Funding: This research was funded by the Key Program of the National Natural Science Foundation of China, grant number 52130607, the Science and Technology Program of Gansu Province, grant number 21JR7RA262 and the Double First-Class Key Program of Gansu Provincial Department of Education, grant number GCJ2022-38.

Institutional Review Board Statement: Not applicable.

Informed Consent Statement: Not applicable.

Data Availability Statement: Not applicable.

Conflicts of Interest: The authors declare no conflict of interest.

References

1. Tortajada, C.; Biswas, A.K. Water management in post-2020 world. *Int. J. Water Resour. Dev.* **2020**, *36*, 874–878. [CrossRef]
2. Chen, L.; Li, K.; Chen, S.; Wang, X.; Tang, L. Industrial activity, energy structure, and environmental pollution in China. *Energy Econ.* **2021**, *104*, 105633. [CrossRef]
3. Xiao, L.; Liu, J.; Ge, J. Dynamic game in agriculture and industry cross-sectoral water pollution governance in developing countries. *Agric. Water Manag.* **2021**, *243*, 106417. [CrossRef]
4. Chen, C.; Kuang, Y.; Hu, L. Challenges and Opportunities for Solar Evaporation. *Joule* **2019**, *3*, 683–718. [CrossRef]
5. Lord, J.; Thomas, A.; Treat, N.; Forkin, M.; Bain, R.; Dulac, P.; Behroozi, C.H.; Mamutov, T.; Fongheiser, J.; Kobilansky, N.; et al. Global potential for harvesting drinking water from air using solar energy. *Nature* **2021**, *598*, 611–617. [CrossRef] [PubMed]
6. Tu, Y.; Wang, R.; Zhang, Y.; Wang, J. Progress and Expectation of Atmospheric Water Harvesting. *Joule* **2018**, *2*, 1452–1475. [CrossRef]
7. Jänchen, J.; Ackermann, D.; Stach, H.; Brösicke, W. Studies of the water adsorption on Zeolites and modified mesoporous materials for seasonal storage of solar heat. *Sol. Energy* **2004**, *76*, 339–344. [CrossRef]
8. Furukawa, H.; Gándara, F.; Zhang, Y.-B.; Jiang, J.; Queen, W.L.; Hudson, M.R.; Yaghi, O.M. Water Adsorption in Porous Metal–Organic Frameworks and Related Materials. *J. Am. Chem. Soc.* **2014**, *136*, 4369–4381. [CrossRef] [PubMed]
9. Heidari, A.; Roshandel, R.; Vakiloroaya, V. An innovative solar assisted desiccant-based evaporative cooling system for co-production of water and cooling in hot and humid climates. *Energy Convers. Manag.* **2019**, *185*, 396–409. [CrossRef]

10. Sleiti, A.K.; Al-Khawaja, H.; Al-Khawaja, H.; Al-Ali, M. Harvesting water from air using adsorption material—Prototype and experimental results. *Sep. Purif. Technol.* **2021**, *257*, 117921. [CrossRef]
11. Xu, J.; Li, T.; Yan, T.; Wu, S.; Wu, M.; Chao, J.; Huo, X.; Wang, P.; Wang, R. Ultrahigh solar-driven atmospheric water production enabled by scalable rapid-cycling water harvester with vertically aligned nanocomposite sorbent. *Energy Environ. Sci.* **2021**, *14*, 5979–5994. [CrossRef]
12. Lei, C.; Guo, Y.; Guan, W.; Lu, H.; Shi, W.; Yu, G. Polyzwitterionic Hydrogels for Efficient Atmospheric Water Harvesting. *Angew. Chem. Int. Ed.* **2022**, *61*, e202200271. [CrossRef] [PubMed]
13. Kalmutzki, M.J.; Diercks, C.S.; Yaghi, O.M. Metal–Organic Frameworks for Water Harvesting from Air. *Adv. Mater.* **2018**, *30*, 1704304. [CrossRef]
14. Fathieh, F.; Kalmutzki, M.J.; Kapustin, E.A.; Waller, P.J.; Yang, J.; Yaghi, O.M. Practical water production from desert air. *Sci. Adv.* **2018**, *4*, eaat3198. [CrossRef] [PubMed]
15. Hanikel, N.; Prévot, M.S.; Fathieh, F.; Kapustin, E.A.; Lyu, H.; Wang, H.; Diercks, N.J.; Glover, T.G.; Yaghi, O.M. Rapid Cycling and Exceptional Yield in a Metal-Organic Framework Water Harvester. *ACS Cent. Sci.* **2019**, *5*, 1699–1706. [CrossRef]
16. Hu, Y.; Fang, Z.; Wan, X.; Ma, X.; Wang, S.; Fan, S.; Dong, M.; Ye, Z.; Peng, X. Carbon nanotubes decorated hollow metal–organic frameworks for efficient solar-driven atmospheric water harvesting. *Chem. Eng. J.* **2022**, *430*, 133086. [CrossRef]